PERGAMON

Journal of Geodynamics 35 (2003) 425–441

JOURNAL OF GEODYNAMICS

www.elsevier.com/locate/jog

Vertical crustal motion observed in the BIFROST project

Hans-Georg Scherneck[a,*], Jan M. Johansson[a], Hannu Koivula[b], Tonie van Dam[c], James L. Davis[d]

[a]*Chalmers University of Technology, Onsala Space Observatory, SE-439 92 Onsala, Sweden*
[b]*Finnish Geodetic Institute, PL 15, FI-02431 Masala, Finland*
[c]*European Centre for Geodynamics amd Seismology, 19, rue Josy Welter, LU-7256 Walferdange, Grand Duchy of Luxembourg*
[d]*Harvard-Smithsonian Center for Astrophysics, 60 Garden Street, Cambridge, MA 02138, USA*

Abstract

This paper reports from investigations on the robustness of estimated rates of intraplate motion from the continuous GPS project BIFROST (Baseline Inferences from Fennoscandian Rebound Observations, Sealevel and Tectonics). We study loading effects due to ocean, atmosphere and hydrology and their impact on estimated rate parameters. We regularly find the admittance of a modelled perturbation at less than fifty percent of the full effect. We think that the finding relates to a difficult noise situation at all periods, and that a satisfying model for the dominating noise source has not been found yet. An additional reason for low admittance is found in the mapping process of the no-fiducial network solution into a conventional reference frame.

1. Introduction

The BIFROST project was created in 1993 to measure postglacial isostatic adjustment in Fennoscandia with continuous GPS in all three spatial dimensions. The project aims at inference of absolute sea level change by combination of the vertical rates with tide gauge derived relative sea level rates. The project also expects to reveal horizontal motion, maybe at first order due to postglacial rebound, but also possibly due to other sources of stress generally covered under the term of neotectonics or intraplate tectonics. Several publications are available, BIFROST project (1996), Scherneck et al. (1998, 2001, 2002), Milne et al. (2000) and Johansson et al. (2002), that centre on the measurement and its interpretation in terms of models for deglaciation history,

* Corresponding author. Tel.: +46-31-772-5556; fax: +46-31-772-5590.
E-mail address: hgs@oso.chalmers.se (H.-G. Scherneck).

0264-3707/03/$ - see front matter
doi:10.1016/S0264-3707(03)00005-X

earth isostatic adjustment response, and the sea level problem. In this context it appears important to assess the robustness of the rates estimated in the regression analysis. For instance we will have to test their dependence on the presence of time series of modelled or measured perturbations. This will be the main subject of the present paper.

Since the beginning the BIFROST data base contains position estimates from 2500 daily solutions. A typical vertical precision is 7 mm (east 3 mm, north 2 mm). For each of the stations in the data base, time series of position estimates are formed, from which components of motion can be estimated. The question arises what components can be attributed to the physical motion of the tectonic unit, whether components are present due to the monument or the local rock unit, and further what are the components contributing to this motion. Remaining variations of position might then be viewed as measurement errors, and also they are considered as being composed of signals from different origins, e.g. variable antenna phase centre offsets.

1.1. Time series of positions

Daily position estimates have been derived on the basis of a mixed reference system; we have adopted the International Terrestrial Reference Frame ITRF97 for positions and JPL2000 for velocities (see Scherneck et al., 2002, for more detail.) The movement of a rigid frame was subsequently subtracted from the daily positions in order to reduce the motion to an average Eurasian motion. Thus, the relative motion, e.g. due to intraplate deformation, is emphasized while all information relevant for deformation is preserved.

In the following we will concentrate on the vertical. An example for the data series is shown in Fig. 1 for the case of Sundsvall. The question arises as to whether the introduction of bias parameters in the time series for the reduction of antenna phase centre offsets does not interact with essentially unbounded noise so as to make the time series falsely stationary. The only answer we presently can give in this regard is, that our time series are not disturbed by antenna reconfigurations after autumn 1996, when the last bias parameter was introduced. If power-law noise would be present, the three years of data since then should be expected to exhibit the feature in the form of an upward sloping low-frequency asymptote.

Antenna related problems in the BIFROST project were first studied in Elósegui et al. (1995) and Jaldehag et al. (1996a). The findings suggest that non hemispherical covers above the antenna (radomes), mounted for the purpose of protection against environmental perturbations, have a significant impact on the antenna diagram. This leads to changes of the antenna phase centre that depend on satellite elevation, and therefore a dependence of the estimated position on the visible satellite geometry, the horizon mask and/or the elevation cutoff angle (a processing parameter). Further, a snow cover on a radome was found to have a strong influence on the estimated vertical position (Jaldehag et al., 1996b). Some antennas were protected against the incidence of indirect satellite signal, e.g. scattered off from surfaces near the antenna, using radar wave absorbing material (“eccosorb”). An exact position of the eccosorb slab that would lead to perturbation-free antenna diagram is difficult to find, as it again depends on satellite elevation. The task to find neutral receiving conditions involves a large amount of trade-offs and compromises; the changes that occurred in the SWEPOS and FinnRef networks are detailed in Johansson et al. (2002). At every change of the configuration we have to be prepared that the estimated position changes. One of the lessons learnt in the process suggests that a low

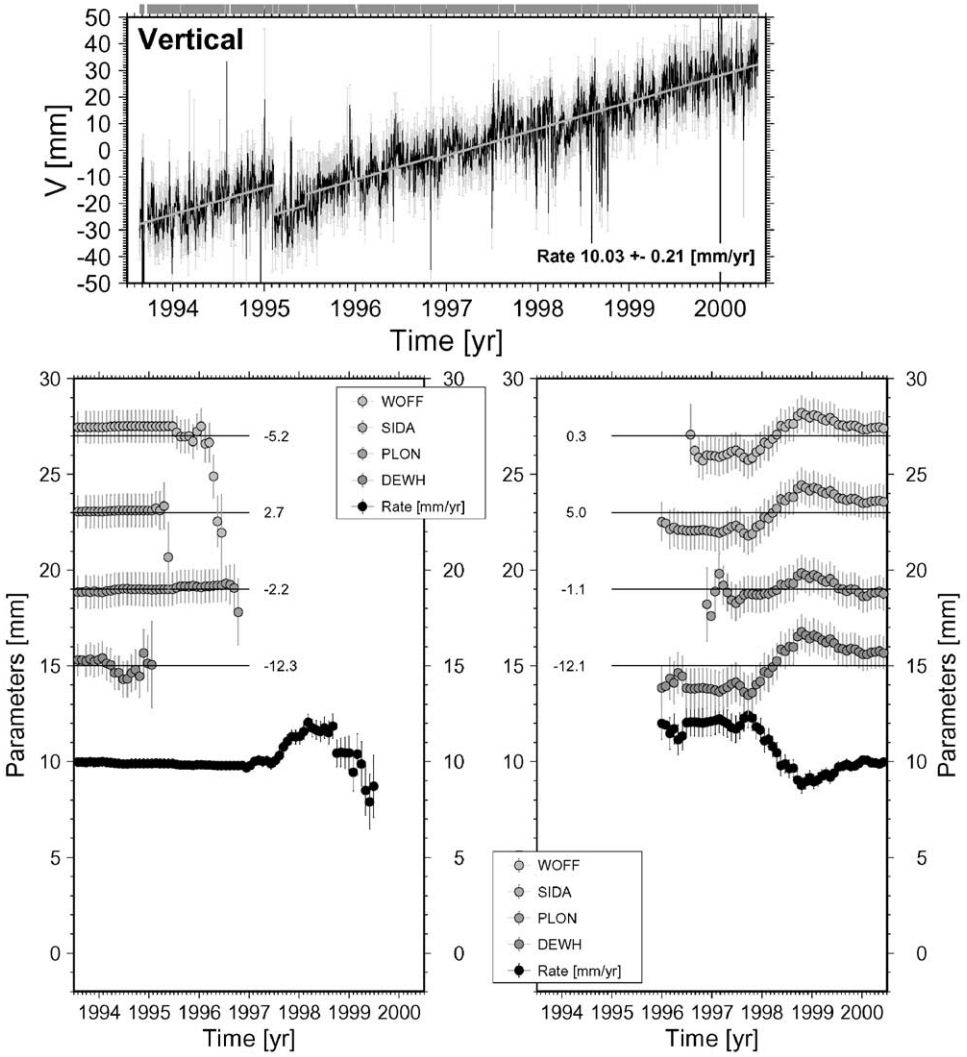

Fig. 1. Top frame: time series of vertical position at Sundsvall (black curve with a gray background that shows the standard deviation of each daily estimate). Fitted simple motion model, consisting of adjusted constant rate and bias parameters is shown as a gray line. The biases are seen as jumps permitted to occur at times when we might expect that changes in antenna configuration could have reverberations on the estimated position, e.g. covering radomes, where changed. Bottom frames: Cutoff test, showing estimated parameters for bias and rate as chunks of 30-day length are chopped off the beginning (lower left) and the end (lower right) of the time series. The antenna radome events are denoted with four-letter codes, see text.

(5°) elevation cutoff angle leads to a more balanced sampling of the antenna sensitivity pattern, given its variations typical in our networks. In lieu of the reprocessing of the GPS data currently carried out at Onsala Space Observatory with the lower elevation cutoff, bias parameters must be introduced in the data analysis when average positions are estimated from the daily solutions.

The introduction of biases interacts with the estimation of a constant rate. By cutting batches with increasing length from the time series, from both the heading and the trailing end, the stability of the rate and bias estimates can be evaluated. Changes of rate estimates can be monitored when a bias time is cut away. The result, again for Sundsvall, is shown in Fig. 1. At this station the following antenna radome reconfigurations were carried out (codes used in the figure in parenthesis). The Delft type radome was changed against a pointed fibreglass "white" type (DEWH). Later, the white radome was removed and operation continued for a short time without radome (WOFF). Finally, a hemispherical Plexiglas radome was installed (PLON) leading to much reduced elevation dependence of the measured satellite range (the previous models were conical). In the southern part of the network this change occurred several months earlier, therefore allowance is given for a side-effect jump (SIDA).

The test results indicate that data from before autumn 1996 could be sacrificed, trading off only a little of the resolution. The cut-off test at the end shows that there is still some drift of the rate during the last twelve-month period, and the present estimate of 10 ± 0.2 mm/year might change by more than one standard deviation. There are stations in the network the trends of which are more difficult to determine in the presence of more antenna jumps and greater long-period noise.

1.2. Concepts to separate motion and measurement error

The standard BIFROST model for motion of a station consists of a constant rate and of biases that are introduced when antenna configuration or receiving conditions have been changed; these signals are conceived of as being embedded in Gauss-Markov noise. The important notion with this kind of noise, in contrast to random walk, is that it possesses a stable mean. If the time span is long enough during which a station is observed, a meaningful mean and lower polynomial orders of a motion model can be estimated. This notion corresponds to the notion of stable, almost rigid tectonic plates. In sediment-covered areas such stability conditions might be difficult to establish (Langbein and Johnson, 1997).

From power spectrum estimation we know that the noise character of our time series to date shows a slope that is far from the $1 = f^2$ of random walk. However, we do not know the spectrum at periods that are as long as or longer than the duration of the experiment. Linear motion generated by a random walk process that fits the noise power at the lowest frequency could be misinterpreted as deterministic. As an exercise for BIFROST, a typical noise power figure at one year period is 500 mm^2 day, which is about 10 dB above the noise power at the Nyquist frequency. The case is illustrated in Fig. 2 for the case of the vertical position estimates at Sundsvall. A random walk spectrum taking off at the Nyquist with 50 mm^2 day would reach $20 \times_{10} \log(365) = 51$ dB at a 1 year period. However, the 500 mm^2 day figure could be indicative of random walk with a process noise parameter of $\sqrt{500}/365 = 0.06$ mm/$\sqrt{\mathrm{d}}$. This noise would be screened by other processes more white in character. In 2500 days, the random walk component could build up an offset of 150 mm, which would be misinterpreted as an average rate of 20 mm per year.

Power-law noise with a less steep character than the $1 = f^2$ slope of random walk is frequently encountered (Williams et al., 2001; Calais, 1999). Although these types of noise are less severe in terms of the long-period drift of the station position, they have in common that they are deficient of a stable mean.

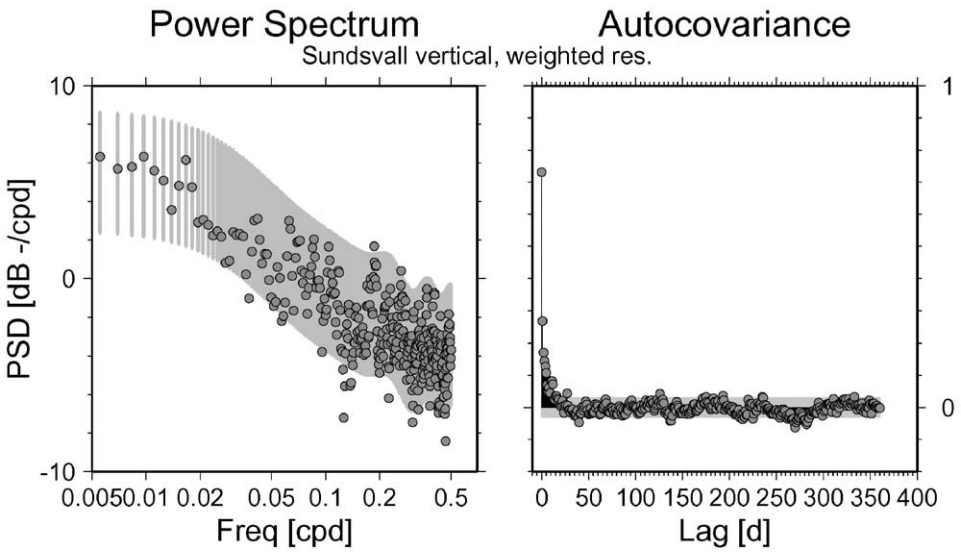

Fig. 2. Power spectrum and auto-covariance at Sundsvall, vertical component. The times series of daily estimates is analysed after reduction of the simple motion model (one constant rate of motion and bias parameters introduced at times of antenna reconfiguration). This motion residual has then been normalised with the standard deviation at every estimate (mean value 7 mm). Thus, zero decibel corresponds to a power spectrum density of 50 mm^2 day. The power spectrum noise colour indicates a Gauss-Markov noise process, as the spectrum appears to saturate at a finite level when the frequency decreases. The Bartlett estimate is denoted by circles. The spectrum has also been estimated using a Maximum Entropy method (MEM). This is shown as a band of vertical bars. The bar length indicates the 95% confidence interval of the Bartlett spectrum. Thus, outliers of the Bartlett spectrum outside this band are significant at the 95% level. We find 15 small outliers out of 720 samples. Only the spectral lines at 0.2 and 0.4 cycles per day, that have been picked up by the MEM, might bear any significance. The auto-covariance series (right frame) indicates a Gauss-Markov parameter of 0.6.

2. Inferred motion

The article by Johansson et al. (2002) describes the three approaches that have been taken in the post-processing of the GPS analysis, inferring three-dimensional crustal motion in Fennoscandia. These results show a high degree of correspondence with predicted motion on the basis of glacial isostatic rebound models (Milne et al., 2001) and contemporary vertical rates of motion relative to the conventional sea level (Ekman, 1996). The new implications in the BIFROST GPS measurements are that the observed motion is truly three-dimensional, and that it aims to relate the motion to the geocentric origin that is maintained by the International Terrestrial Reference System (ITRS) rather than a conventional mean sea level.

In the standard BIFROST solution, we reduce the time series for loading effects due to air pressure and fit sinusoidal harmonics with annual and sub-annual signatures up to four cycles per year, as these effects are both straight-forward to model and visually discernable in the resulting time series. At various degrees of sophistication several stations have obtained extended site motion models. For instance, near the Baltic Sea coast, loading due to the varying water level of the sea is considered. Using an Empirical Orthogonal Function (EOF) approach, we also consider a stochastic portion of motion to be more or less in common at all stations in an area. In

Fig. 3 we show a map produced from the three-dimensional rates of motion determined with the EOF-method where possible (all stations in Sweden and Metsähovi). Elsewhere a solution with automated outlier editing using a criterion of five standard deviations is used.

2.1. Vertical motions compared with tide gauges and leveling

We show two variants of comparison of the GPS results with vertical rates determined from tide gauges and precise levelling, first with the EOF-solution, second with the standard solution (Fig. 4). We use the tide gauge and levelling results of Ekman (1996) and add the geoid motion due to the rebound model of Mitrovica et al. (1994). In both cases, GPS and tide gauge/levelling, we obtain the geometric rate of motion of the earth surface. In the case of GPS the motion is relative to the centre of the satellite frame, which is constrained to the earth's gravity centre (how well remains to be determined). In the case of tide gauge/levelling the reference is the regional sea

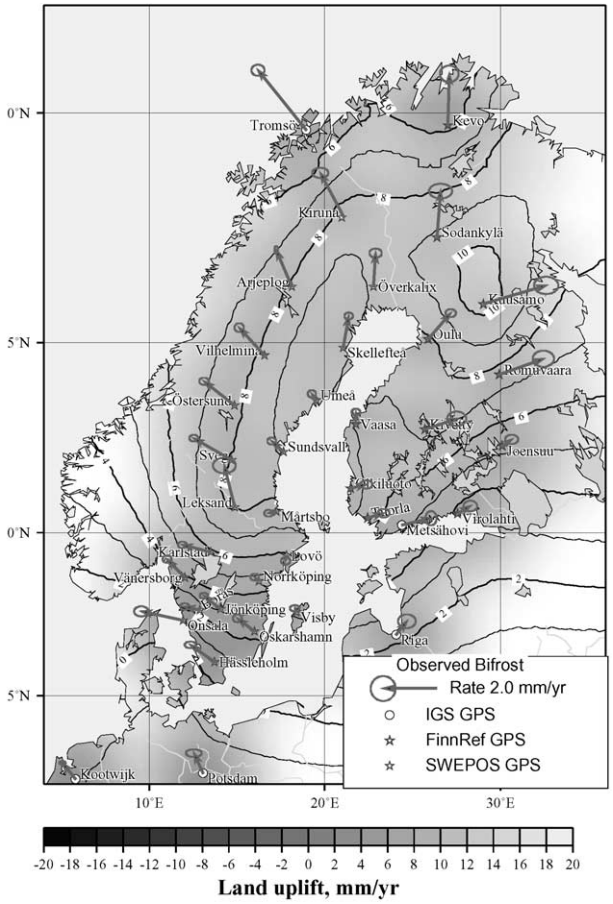

Fig. 3. Three-dimensional rates, vertical rates plotted as colours, horizontal rates as arrows with error ellipses for one standard deviation. The vertical standard deviation is typically 0.25–0.35 mm/year in Sweden; the somewhat shorter observation time span in Finland causes error limits near 0.5 mm/year.

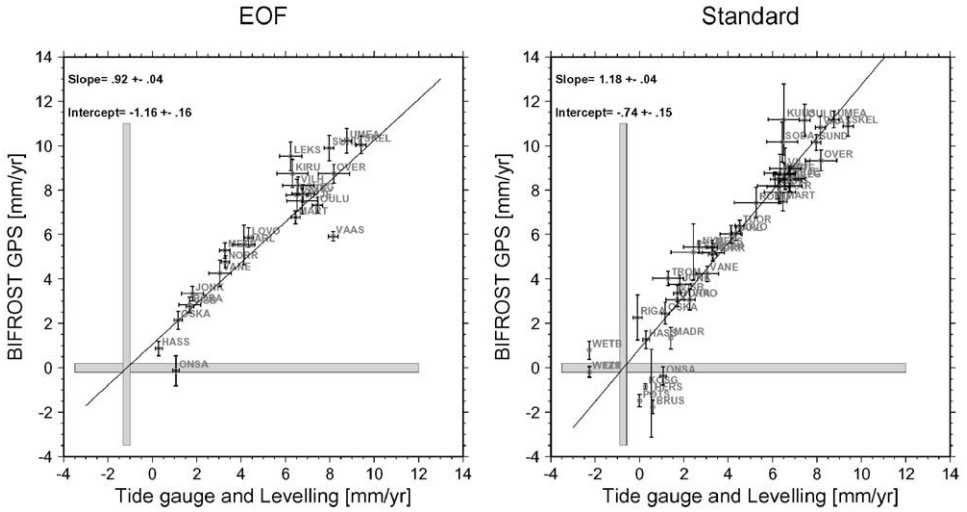

Fig. 4. Regression of GPS derived vertical motion with respect to motion inferred from tide gauges and precise levelling (Ekman, 1996). Tide gauge readings and levelling are reckoned relative to a changing sea level, while GPS refers to the mass centre of the Earth. Thus, the intercept of both curves indicates the rate of the relative vertical motion of the land surface reduced for postglacial rebound as a regional average. The negative of this figure hints at the regional change of sea level reduced for the postglacial land motion. A perfect fit to a straight line with unity slope would indicate that the sea level rise is uniform. In the left frame only the GPS results from the stations with the longest records have been used, and the empirical orthogonal function method has been used to remove common modes of noise. In the right frame the BIFROST standard solution has been used, where station motion is modelled as one rate and biases as required. The motion solutions are described in Johansson et al. (2002).

surface. The difference between the two data sets interpolated to the point where GPS motion, i.e. inferred land surface motion is zero determines the regional change of sea level with respect to the earth's gravity centre.

Where no tide gauge/levelling data is available from Ekman (1996), which is the case at many IGS stations, we resort to ITRF97 motions. In the case of Ny Ålesund (NYAL) a careful evaluation of mareograph data was presented by Breuer and Wolf (1995), who estimated a relative uplift velocity of 2.6 ± 0.7 mm/yr. The ITRF97 motions have been excepted from computing the regression line shown in Fig. 4. More discussion on this subject follows in Section 4.

3. Loading effects

Recently, global hydrological data was used by van Dam et al. (2001) to predict loading induced displacements of the earth surface. We apply the method to predict displacements at the set of BIFROST GPS stations.

Storage of water in snow cover, soil, and groundwater was calculated using a global model of land water and energy balance (Milly and Shmakin, 2002a). Summation of model water storage outputs (snow, soil water and groundwater) provides our estimate of terrestrial water storage loading on a monthly time scale at 1° by 1° global spacing.

The atmospheric pressure data set consists of 6-h estimates of surface pressure determined by the European Centre for Medium Range Weather Forecast (ECMWF). The data are retrieved from spherical harmonic developments up to degree and order 213 and represented globally on a 1° by 1° grid.

For both the atmospheric pressure and continental water storage loading estimates, the mass was convolved with Farrell's elastic Green's functions (Farrell, 1972). The procedure has been described in detail in van Dam and Wahr (1987).

Time series for the case of Östersund are shown in Fig. 5. This station is a good example for the impact of severe snow winters. The hydrological loading predictions are available for a time period between January 1994 and December 1998. We have also acquired soil moisture and snow coverage data observed in a network of climate monitoring stations operated by the Swedish Meteorological and Hydrological Institute (SMHI). This data covers the period from January 1996 to date. Although these measurements of soil moisture and snow height are local, correlation between the stations in the network is generally high over distances of several hundred kilometres. For this reason we think that they are representative of the hydrological budget in the ground. In contrast to the Milly and Shmakin (2002a) model, which makes detailed assumptions of vegetation related parameters (Milly and Shmakin, 2002b), the SMHI data does not include the water bound in vegetation over ground.

To convert the local observations into predicted loading effects we have used a coefficient of −0.03 m per metre of water column. This coefficient has been obtained by convolving typical mass distributions with an elastic Greens function (Farrell, 1972), see Fig. 6. The SMHI hydrology time series are for snow and soil are added to form a loading-efficient time series. The series with the snow alone is included in the regression with the GPS observations, since other effects of snow, e.g. average effects on the wave propagation, might be reduced in this way. A comparison of both time series during the 3 years overlap shows that the typical summer water storage peak appears generally low in the local soil measurements compared to the soil and vegetation model.

With respect to the daily GPS solutions the loading effects can be regarded as quasi-static. Therefore we consider only one in-phase admittance coefficient for each of the perturbing effects. Unfortunately, the atmospheric load and the hydrological load compete at annual frequencies, while the atmospheric load—quite uniquely—has substantial variations also on a weekly scale. In this short period range we think that, besides the barometrically and tidally incurred displacements, only atmospheric perturbations of signal propagation and multipath would affect the GPS derived positions.

A typical result for atmospheric loading that we have found before hydrological loading was considered ranges between 0.2 and 0.35 for the ratio between the observed and the predicted effect. The admittance does not change significantly when the Gauss-Markov noise parameter is varied over a wide range of values.

When we use the hydrological loading predictions from the global convolution we find admittance coefficients below unity (cf. Table 1). As an alternative we have used the soil moisture data from the SMHI Climate Stations operated by the Swedish Meteorological and Hydrological Institute (SMHI). For these time series typically a very low admittance is found. In each case we explain the deficiency as follows in the discussion. The estimated admittance coefficients for hydrological loading at stations in northern Sweden are shown in Fig. 7.

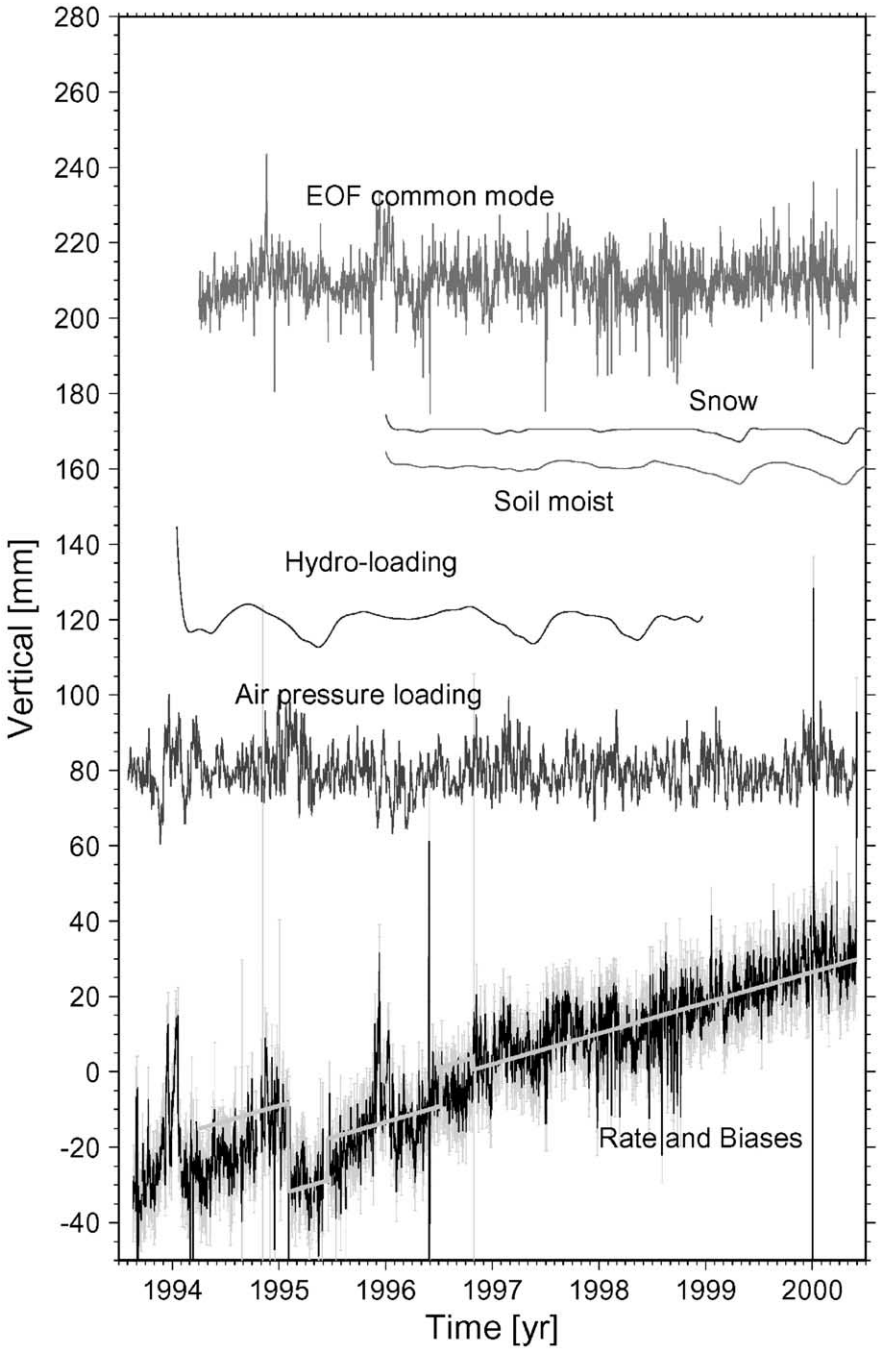

Fig. 5. Time series at Östersund, vertical component. The observed variation of position is dominated by postglacial rebound. Observations are shown in the bottom curve together with standard deviations. The the series labeled hydro-loading is computed from Milly and Shmakin (2002a) using global convolution; the soil (-moisture) and snow curves are predicted using local observations and a coefficient of −0.03. The conditions are typical also for the other stations especially in northern Sweden.

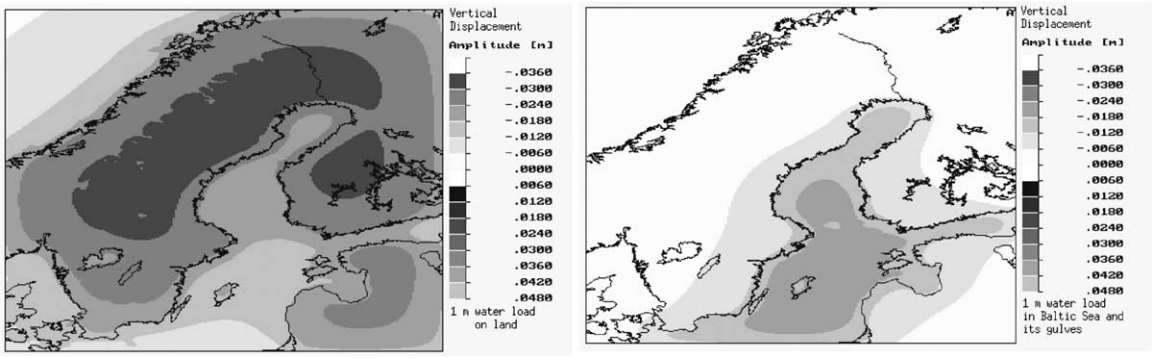

Fig. 6. Loading effects due to a uniform slab of 1 m water separately covering the land part (left frame) and the sea part (right frame) of the Fennoscandian shield.

Table 1
GPS vertical position variations, admittance coefficients for predicted hydrological loading effects according to van Dam et al. (2001)

Site	Coeff.	S.D.	Comment
ARJE	0.974	0.098	
JONK	0.408	0.133	
KIRU	0.005	0.092	LOW
MART	0.304	0.120	
OSKA	−0.234	0.215	CONTRA
VANE	0.577	0.157	
OVER	0.664	0.107	
SUND	0.565	0.114	
SVEG	0.723	0.089	
UMEA	1.016	0.101	
VILH	0.909	0.088	

4. Discussion

We start the discussion with a look at the comparison of the motion inferred from tide gauge observations and precise levelling to the GPS observations (see Fig. 4). The graph indicates a regional mean sea level change. How- ever, we obtain different results depending on the post-processing analysis strategy, the simple standard analysis versus the empirical orthogonal function analysis (described in Johansson et al., 2002). Clearly the sea level rate that might be inferred depends upon data quality or data processing related features. Although the error bars in this figure have been derived from the a posteriori residuals and adjusted for noise colour, the difference between the solutions is significant at almost three standard deviations. The analysis to date suggests so far that a sea level rate based on BIFROST GPS is not sufficiently robust, hence premature, and that the confidence limit of 0.15 mm/year is over-optimistic. Tentatively, the methods that treat the data more homogeneously and that have an enhanced capability to sepa-

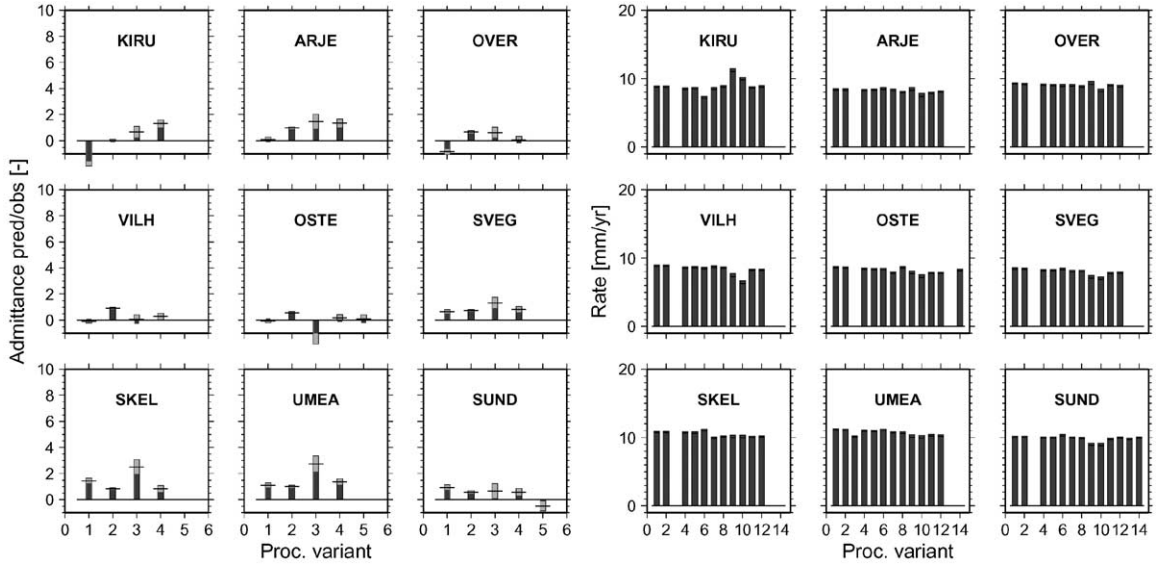

Fig. 7. Estimated admittance coefficients for observed versus predicted hydrological loading effects (leftmost nine frames) and the vertical rate parameters solved for a number of processing variants (rightmost nine frames). The processing variants are explained in Tables 2 and 3.

rate signal from noise, that is the EOF method, could be interpreted as more reliable, and so would be their result, a sea level rate slightly in excess of 1 mm/year. Removing observations under snow conditions from the post-processing, Scherneck et al. (2002) arrived at a sea level rate closer to 1.5 mm/year. Thus, there is a continuing interest to understand the systematic effects that perturb the measurement and that so far have been treated as noise.

Interesting candidates in this context are the loading effects. The associated signals in our time series can be considered as being spatially coherent over large distances. This spatial coherence could be seen as an effect of the elastic stiffness of the mantle. However, the extent of the coherence also happens to be on the order of the diameter of the load distribution, typically involving scales of 200–1000 km (ocean basins, weather systems, the continental landmass of Fennoscandia).

The GPS network solution uses a seven-parameter transform in order to map the daily position solutions into a conventional, International Terrestrial Reference Frame (ITRF). At the stage of mapping the loading model has not been applied (except for global tide and ocean tide loading). The mapping is a time-consuming task and results in a space-consuming product, leaving little room to experiment. The mapping attenuates the local displacements at the controlling sites because the associated equation system is over-determined. Thus, the time-series that is obtained at these stations may look ''better than true''. This might explain the very low barometric loading admittance (less than 10% of the theoretical value) found at these sites (cf. Fig. 8, especially METS, Metsähovi).

Hydrological loading and atmospheric pressure loading occur simultaneously. Now, if both effects are realistically modelled and the data is affected by both of these effects, their admittance coefficients ought to become larger. However, our findings seem to suggest that long-period loading due to hydrology is admitted by trading off the more wide-band barometric loading. This

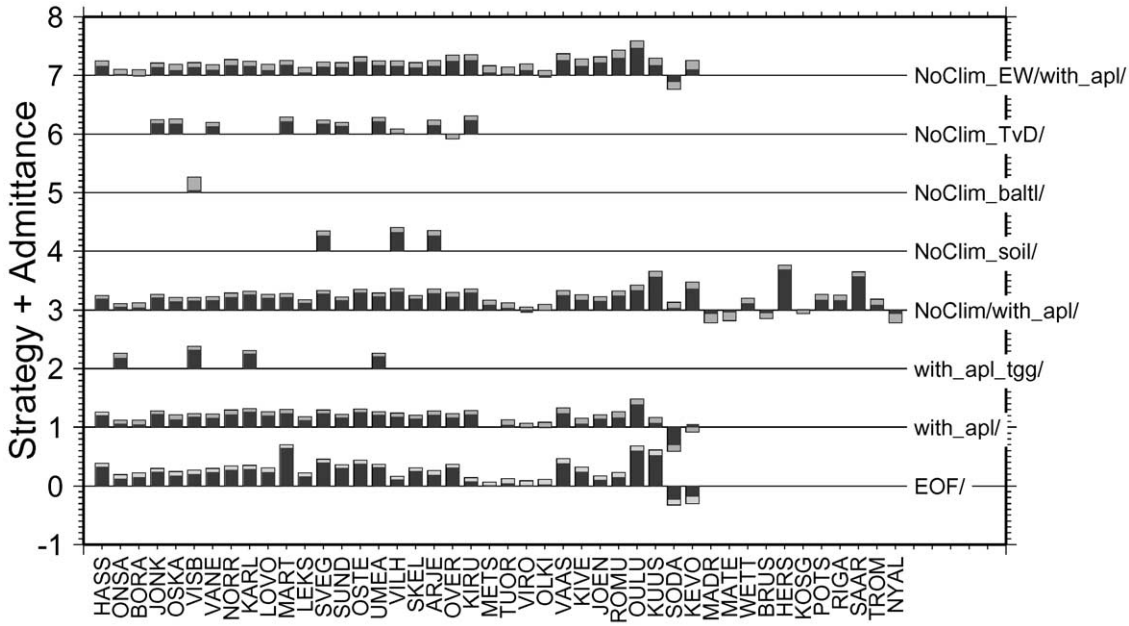

Fig. 8. Air pressure loading, admittance coefficients at each station in a range of processing variants. The different processing options—linear regression of a variety of environmental parameters—are denoted as follows: NoClim, no seasonal cycles estimated; _apl, include air pressure loading; _tgg, include tide gauge record; _baltl, Baltic loading, i.e. combined air pressure and sea level; _soil, include SMHI soil moisture; _TvD, include hydrologic loading (van Dam et al., 2001); _EW, data during winter months are suppressed. The admittance coefficient is represented by the height of the dark-gray bar, its uncertainty by the height of the light-gray cap.

is the more surprising as the spatial coherence of atmospheric variations is expected to be more narrow, and thus we would expect each station to move in more or less unique patterns, while hydrological loading would generate signals that are coherent over greater wavelengths.

Adding sea level loading to the analysis, the region affected on land is much smaller than in the case of hydrological loading. The effect has an strong negative correlation with air pressure loading at the open ocean. The Baltic Sea is a semi-enclosed basin and responds only slowly to pressure changes. Still, on the long term the anti-correlation is not negligible. Adding these time series in the regression, the admittance for all effects in the model is again expected to rise. This is indeed observed (see Tables 2 and 3).

The low admittance in the SMHI soil moisture case is probably a consequence of the signal variation being dominated by snow effects. Snow on the radome that covers the antenna and subsequently changes its electrical characteristics leads generally to a positive height change of the phase centre. Thus, it is sign-opposed to the loading effect, and it is regularly found at one order of magnitude greater. Snow conditions on an antenna at a GPS station and the amount of snow on the ground at a climate station several tens of kilometres apart do not necessarily correlate very well. In the snow-free parts of the year, the loading effect due to soil moisture might prevail. But also here ground reflectivity and scattering and absorption in vegetation near the antenna might have an electrical effect on the observed antenna position.

Table 2
Processing options for hydrological loading used in Fig. 7

1	global convolution, S = no
2	like 2, S = yes
3	local soil moisture observations, S = no
4	like 3, S = yes
5	like 3, S = yes, EOF-method

"S" denotes simultaneous estimation of seasonal sinusoids. Simultaneous air pressure loading is always considered. In the fit to the GPS observations, simple regression is used unless EOF denotes when the Empirical Orthogonal Function method has been used. Global convolution uses the predictions from van Dam et al., 2001, local soil moisture uses the observations from SMHI.

Table 3
Processing variants for rate estimation

1	standard analysis, AP = no, S = yes
2	like 1, with AP
3	like 2, with tide gauge
4	like 1, but S = no
5	like 4, with AP
6	Summer-only solution (Scherneck et al., 2002) with AP
7	like 2, H = LO, S = yes
8	like 2, H = LO, S = no
9	like 5, H = GC, S = yes
10	like 5, H = GC, S = no
11	EOF, S = yes
12	like 11, with AP
13	like 11, H = LO
14	like 11, with AP, H = LO

Here, different loading scenarios are played through, e.g. air pressure loading (AP) with and without simultaneous hydrology (H), and hydrology represented by global convolution (H = GC) or local observation (H = LO). Estimation of seasonal cycles is denoted by "S".

Visby (VISB) on the island of Gotland presents an interesting case in Fig. 8. When the loading from air pressure and sea level are combined, giving approximately a sea bottom pressure, the remaining air pressure loading effect has an insignificant amplitude. The effect to be admitted is supposed to consist of the pressure acting on the island only, which is expected to cause only little additional deformation.

First attempts to discriminate loading effects due to variations in the Gulf of Bothnia and Baltic Sea level reveals low admittance again by a factor of three to four. Table 4 shows admittance coefficients of vertical position versus water level at the closest tide gauge. These values are typically close to −0.004, whereas Fig. 6 suggests coefficients between −0.01 and −0.02. In particular, the Gulf of Bothnia has some unique features that are not expected to correlate with perturbations at IGS stations (even not Metsähovi, the closest station). The basin is small, is subject to a changing supply in the freshwater catchment area, and on the short time scale, large excursions from equilibrium (typically at 0.3 m range) can occur because of its dynamic response to the wind field. The low sensitivity of the GPS station vertical to sea level loading contradicts our favourite

Table 4
GPS vertical position variations, admittance coefficients for regional sea level

Site	Coeff.	S.D.	Tide gauge	Pressure loading	
				w/o	with tide gauge
ONSA	−0.0041	0.0012	Ringhals	0.17	0.25
KARL	−0.0056	0.0009	Lake Vänern	0.29	0.29
VISB	−0.0109	0.0011		0.20	0.33
OSKA	−0.0036	0.0011		0.17	0.23
SUND	−0.0059	0.0009	Spikarna	0.21	0.20
UMEA	−0.0020	0.0008	Ratan	0.24	0.29
SKEL	−0.0034	0.0008	Furuögrund	0.17	0.25

Theoretical coefficient is between −0.01 and −0.03. Pressure loading coefficients represent admittance of predicted effect. Their typical standard deviation is 0.03.

explanation for low admittance for air pressure loading, namely the long-wavelength correlation of these parameters and the neglected influence of the effect at the IGS stations (in orbit computation as well as during mapping of regional results into the reference frame).

Our investigation on the dependence of the rate parameter on different processing options seems to indicate that (1) data from before autumn 1996 do not contribute significantly to the robustness of the estimates. Thus the early years of the project could soon be ignored in the estimation of motion; during this period most of the changes of the antenna assemblies had occurred, necessitating the estimation of many bias parameters. (2) The loading effects that we have studied are not vital for the robustness of rate estimates. Most of the variations shown in Fig. 7 are within one standard deviation.

The largest changes can be seen in the variants 9 and 10. They include the hydrological loading from the global convolution of the Milly and Shmakin (2002a) data set (van Dam et al., 2001). The change in the rate, however, is possibly a consequence of the truncation of the time series analysis at the end of the year 1998. This notion is supported by the end-cutoff test shown in Fig. 1. From Fig. 8 we find that the admittance of hydrological loading trades off with the admittance of atmospheric pressure loading. This could be interpreted as a competitive process about mostly the annual period in the observations. An annual period in GPS data, however, may collect many more effects than those considered in this study.

Fig. 5 includes the EOF common mode. Like in the example shown, we regularly find that this signal contains roughly 50% of the of the observation residual as measured by the RMS. The EOF common mode shown has been derived in an extended solution with all perturbing processes included in the signal model (hydrology from SMHI observations). This finding is interpreted as a large degree of the perturbations at one station being correlated in a wide region, and the loading effects due to atmosphere and hydrology (eventually including sea level) do not reduce the residual more than marginally.

The hydrological loading time series, global convolution (van Dam et al., 2001) versus SMHI local observation, are found to differ in their signal content. The SMHI data shows generally less variation. The reason may be that the soil is not the only storage volume for meteoric water. The van Dam et al. (2001) data shows a loading effect at the level of centimetres. If this signal range is

realistic the parameter has the potential to impact the estimated rates, especially if the non-annual components undergo changes, or if secular terms exist. However, extended modeling and testing is needed in order to draw more definitive conclusions.

5. Conclusions

Loading effects of different kinds, air pressure, sea level and hydrology, appear to be resolvable in BIFROST GPS data. In all cases the admittance coefficients found are small on average, smaller than the modelled deformation. The situation for hydrology is especially complicated since the effect of snow on the GPS antennas is twofold, depression due to loading of the crust, and a virtual uplift due to electrical effects.

Our estimated velocities come from a network solution which implies a mapping into the velocity field of a global terrestrial reference system. The connection between these systems is maintained by a few, reliable IGS stations in the larger region. Biases due to correlated long-term noise perturbation can be attenuated with the reduction of a common mode. The common mode can be obtained with an Empirical Orthogonal function method using the longest records.

We certainly can conclude that many perturbing effects are visible in the data. Hydrological loading appears to have a mid but nevertheless significant impact, and it appears necessary to include this signal in the estimation of vertical motion. The present BIFROST solutions used for inference of crustal motion and regional sea level rise have ignored some of the perturbing effects since data availability would lead to truncation of the GPS data. The relatively low admittance coefficients found seem to indicate that the system fends off the perturbations. We can present two explanations. First, large scale effects that affect the region correlate with the motions at the constraining stations; the network solution of a station is the difference of the motion with respect to an effective mean motion of the constraining stations. Second, the reduction of noise in the time series in terms of attenuation is not overwhelming. We think that a combination of effects on the signal side that are difficult to model, higher-order atmospheric propagation perturbations, multipath and scattering are the reason. Thus, explicit and improved modelling in the first phases of the analysis process is the general route to lower noise. All this appears as a process of many small steps rather than expecting a major breakthrough. Improvements that are feasible include: computation of orbits and site positions in a consistent way, taking full advantage of the station density in the area; and elevation masks as low as possible.

Acknowledgements

We thank Sten Bergström and Nils Gustavsson at SMHI for their help with ECMWF pressure and SMHI climate data. Knut and Alice Wallenberg's Foundation and the Swedish Council for Planning and Coordination of Research (FRN) have supported us with equipment. We also thank the National Land Survey of Sweden, especially the staff engaged in the establishment, maintenance, and operation of SWEPOS. Some stations in Finland were created with the support of Posiva OY. In campaigns we used equipment made available by the University Navstar Consortium (UNAVCO). We also acknowledge the support given be the Swedish Research and

Testing Institute (SP). Research projects have been funded by the Swedish Natural Science Research Council (NFR) under project accounts G-AA/GU04770, continued by The Swedish Research Council (SRC) under R 504-15/2001, the Swedish National Space Board (SNSB) under Dnr 171/98, and the Swedish Research Council for Engineering Sciences (TFR). Some figures were generated with the Generic Mapping Tools (Wessel and Smith, 1998). Finally our sincere thanks to the ones that reviewed this work and helped improve the manuscript.

References

BIFROST Project 1996 (R.A. Bennett, T.R. Carlsson, T.M. Carlsson, R. Chen, J.L. Davis, M. Ekman, G. El-gered, P. Elósegui, G. Hedling, R.T.K. Jaldehag, P.O.J. Jarlemark, J.M. Johansson, B. Jonsson, J. Kakkuri, H. Koivula, G.A. Milne, J.X. Mitrovica, B.I. Nilsson, M. Ollikainen, M. Paunonen, M. Poutanen, R.N. Pyskly-wec, B.O. Rönnäng, H.-G. Scherneck, I.I. Shapiro, and M. Vermeer), 1996. GPS Measurements to Constrain Geo-dynamic Processes in Fennoscandia. EOS, Trans. AGU 77, 337–341.

Breuer, D., Wolf, D., 1995. Deglacial land emergence and lateral upper-mantle heterogeneity in the Svalbard archipelago—I. First results for simple load models. Geophys. J. Int. 121, 775–788.

Calais, E., 1999. Continuous GPS measurements across the Western Alps, 1996-1998. Geophys. J. Int. 138, 221–230.

Ekman, M., 1996. A consistent map of the post glacial uplift of Fennoscandia. Terra Nova 8, 158–165.

Elòsegui, P., Davis, J.L., Jaldehag, R.T.K., Johansson, J.M., Niell, A.E., Shapiro, I.I., 1995. Geodesy using the Global Positioning System: the effects of signal scattering on estimates of site position. J. Geophys. Res. 100, 9921–9934.

Farrell, W.E., 1972. Deformation of the Earth by surface loads. Rev. of Geophys. 10, 761–797.

Jaldehag, R.T.K., Johansson, J.M., Elòsegui, P., Davis, J.L., Niell, A.E., Rnnng, B.O., Shapiro, I.I., 1996a. Geodesy using the Swedish permanent GPS network: effects of signal scattering on estimates of relative site positions. J. Geophys. Res. 101, 17–841-17,860.

Jaldehag, R.T.K., Johansson, J.M., Davis, J.L., Elsegui, P., 1996b. Geodesy using the Swedish permanent GPS network: effects of snow accumulation on estimates of site positions. Geophys. Res. Letters 23, 1601–1604.

Johansson, J.M., Davis, J.L., Scherneck, H.-G., Milne, G.A., Vermeer, M., Mitrovica, J.X., Bennett, R.A., El-gered, G., Elösegui, P., Koivula, H., Poutanen, M., Rönnäng, B.O., Shapiro, I.I., 2002. Continuous GPS measurements of postglacial adjustment in Fennoscandia, 1. Geodetic results. J. Geophys. Res. 107, 28. (DOI 10.1029/2001JB000400).

Langbein, J., Johnson, H., 1997. Correlated errors in geodetic time series; implications for time-dependent deformation. J. Geophys. Res. 102, 591–604.

Milly, P.C.D., Shmakin, A.B., 2002a. Global modelling of land water and energy balances: I. The land dynamics (LaD) model. J. Hydrometeorology 3, 283–299.

Milly, P.C.D., Shmakin, A.B., 2002b. Global modelling of land water and energy balances: II. Land-characteristic contributions to spatial variability. J. Hydrometeorology 3, 301–310.

Milne, G.A., Davis, J.L., Mitrovica, J.X., Scherneck, H.-G., Johansson, J.M., Vermeer, M., Koivula, H., 2001. A map of 3-D crustal deformation in Fennoscandia emerges from a network of GPS measurements. Science 291, 2382–2385.

Mitrovica, J.X., Davis, J.L., Shapiro, I.I., 1994. A spectral formalism for computing three-dimensional defor-mations due to surface loads, 2. Present-day glacial isostatic adjustment. J. Geophys. Res. 99, 7075–7101.

Scherneck, H.-G., Johansson, J.M., Elgered, G., Davis, J.L., Jonsson, B., Hedling, G., Koivula, H., Ollikainen, M., Poutanen, M., Vermeer, M., Mitrovica, J.X., Milne, G.A., 2002. BIFROST: observing the three-dimensional deformation of Fennoscandia. In: Mitro-vica, J.X., Vermeersen, B.L.A. (Eds.), Glacial Isostatic Adjustment and the Earth System. Geodynamics Series, Vol. 29, American Geophysical Union, Washington, DC, pp. 69–93.

Scherneck, H.-G., Johansson, J.M., Mitrovica, J.X., Davis, J.L., 1998. The BIFROST project: GPS determined 3-D displacement rates in Fennoscandia from 800 days of continuous observations in the SWEPOS network. Tectonophysics 294, 305–321.

Scherneck, H.-G., Johansson, J.M., Vermeer, M., Davis, J.L., Milne, G.A., Mitrovica, J.X., 2001. BIFROST Project: 3-D crustal deformation rates derived from GPS confirm postglacial rebound in Fennoscandia. Earth Planets Space 53, 703–708.

van Dam, T.M., Wahr, J., 1987. Displacements of the Earth's surface due to atmospheric loading: effects on gravity and baseline measurements. J. Geophys. Res. 92, 1281–1286.

van Dam, T.M., Wahr, J., Milly, P.C.D., Shmakin, A.B., Blewitt, G., Lavallée, D., Larson, K.M., 2001. Crustal displacements due to continental water loading. Geophys. Res. Letters 28, 651–654.

Wessel, P., Smith, W.H.F., 1998. New, improved version of the Generic Mapping Tools released. EOS Trans. AGU 79, 579.

Williams, S.D.P., Baker, T.F., Jeffreys, G. 2001. Coloured noise and annually repeating signals in GPS and gravity time. Geophys. Res. Abstr. CD-ROM, 3, Session G3.02, p. 1628. European Geophysical Society, Copernicus Gesellschaft, Katlenburg-Lindau, Germany.